ARTICLE

Nano-Fe$_3$O$_4$@SiO$_2$-SO$_3$H: A magnetic, reusable solid-acid catalyst for solvent-free reduction of oximes to amines with the NaBH$_3$CN/ZrCl$_4$ system

Leila Sadighnia [ID] | Behzad Zeynizadeh [ID] | Shiva Karami | Mohammad Abdollahi

Faculty of Chemistry, Urmia University,
Urmia 5756151818, Iran

Correspondence
Leila Sadighnia, Faculty of Chemistry, Urmia
University, Urmia 5756151818, Iran.
Email: l_sadignia80@yahoo.com

Funding information
Research Council of Urmia University

In this study, the immobilization of sulfonic acid on silica-layered magnetite was carried out by the reaction of ClSO$_3$H with silica-layered magnetite. The prepared magnetic nanoparticles of Fe$_3$O$_4$@SiO$_2$-SO$_3$H were then characterized using scanning electron microscopy, energy dispersive X-ray spectroscopy, X-ray diffraction, Fourier transform infrared spectroscopy, vibrating sample magnetometry, and transmission electron microscopy. The sulfonated nanocomposite exhibited excellent catalytic activity and reusability in the reduction of various aldoximes and ketoximes with NaBH$_3$CN in the presence of ZrCl$_4$. All reactions were carried out under solvent-free conditions (r.t. or 75–80°C) within 3–70 min to afford amines in high to excellent yields.

KEYWORDS

amines, Fe$_3$O$_4$@SiO$_2$-SO$_3$H, NaBH$_3$CN, oximes, reduction, ZrCl$_4$

1 | INTRODUCTION

Reduction of functional groups plays an important role in the production of a large variety of intermediates in industry and laboratory experiments. In this context, hydride transferring agents derived from the element boron were frequently used for the reduction of functional groups.[1–4] Sodium borohydride as a mild reducing agent has been recognized as the reagent of choice to reduce carbonyl compounds, acyl chlorides, thiol esters, and imines in protic solvents.[5] Currently, the application of NaBH$_4$ is significantly increasing, and hundreds of substituted hydroborate agents have been introduced to control the reducing power of this reagent.[6] Consequently, NaBH$_3$CN as a modified and remarkable resistant hydroborate agent in strong acidic media was also widely used in chemical processes for the reduction of various organic molecules.[7–11]

On the other hand, reduction of oximes to amines is a subject of more interest because oximes are stable derivatives of carbonyl compounds and their subsequent reduction to amines is an attractive two-step procedure for the reductive amination of carbonyl compounds.[12] A literature review shows that most of the reported protocols in this context suffer from some drawbacks. Overcoming the limitations always requires the development and introduction of more efficient protocols using green and benign reaction conditions.

NaBH$_3$CN, carrying an electron-withdrawing cyanide group, is one of the few borohydrides that tolerates strong acidic media. Because of the cyano group, the reducing power of NaBH$_3$CN greatly varies with pH and the adequate reduction rates are obtained only under pH 3–4.[13,14] Under acidic conditions, NaBH$_3$CN reduces oximes to the corresponding hydroxylamines without over-reduction to primary amines.[14] It is also notable that by using strong acidic media, the restriction to use acid-sensitive functional groups is arrived in synthetic organic chemistry. As a solution and to the complete reduction of oximes to amines, the combination of NaBH$_3$CN with the nano-Fe$_3$O$_4$/ZrCl$_4$ system at

solvent-free condition was recently reported by our research group.[15]

In line with the outlined strategies, and in continuation of our research program to explore the reducing capability of NaBH₃CN in the absence of strongly acidic media as well under mild reaction conditions, here we introduce magnetic nanoparticles of Fe₃O₄@SiO₂-SO₃H as a heterogeneous solid-acid catalyst for the solvent-free reduction of various aldoximes and ketoximes to the corresponding primary amines with the NaBH₃CN/ZrCl₄ system (Scheme 1).

2 | RESULTS AND DISCUSSION

Because of the great importance of amines in the synthesis of fine chemicals such as agrochemicals, pharmaceuticals, polymers, dyes, pesticides, photographic, antioxidants, and corrosion inhibitors,[16–20] special attention has been devoted to the preparation of amines.[21,22] Reduction of oximes to the primary amines with hydroborates is one of the most important and practical methods for the preparation of amines. Moreover, the principles of green chemistry calls for new reaction conditions and chemical processes with the advantages in product selectivity, operational simplicity, reusability of the applied catalyst, health, and environmental safety.[23] In the area of catalyst recyclability and reusability, great efforts have been made in the use of magnetic nanoparticles (MNPs). The catalysts incorporated with magnetic species can be easily separated from the reaction mixture using an external magnetic field.[24] Magnetic separation eliminates the need for traditional filtration or other inappropriate procedures for recycling precious catalysts.[25–28] In addition, the modification of magnetic nanoparticles via surface functionalization is an elegant way to bridge homogeneous and heterogeneous catalysts and prevent the particles from aggregation.[29,30] In this context, the development of silica-layered magnetite nanoparticles has attracted the attention of chemists as an excellent catalyst support in many chemical processes.[31,32]

In following up the mentioned strategies and in continuation of our research program toward increasing the reducing power of NaBH₃CN by solid-acid promoters rather than using strenuous acidic solutions, we were prompted to study the acidity influence of the core–shell magnetic nanoparticles of Fe₃O₄@SiO₂-SO₃H in the cyanoborohydride reduction of oximes to amines under mild conditions. The starting point was the synthesis of Fe₃O₄@SiO₂-SO₃H MNPs according to reported procedures.[33,34] The prepared nanocatalyst was then characterized using scanning electron
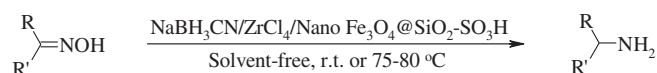
microscopy (SEM), energy dispersive X-ray spectroscopy (EDX), X-ray diffraction (XRD), Fourier transform infrared spectroscopy (FT-IR), vibrating sample magnetometry (VSM), and transmission electron microscopy, and TEM analyses.

The surface morphology and size distribution of the prepared Fe₃O₄, Fe₃O₄@SiO₂ and Fe₃O₄@SiO₂-SO₃H MNPs were determined using SEM. The obtained SEM images show that the prepared nanoparticles are granular with the average size of 23 nm (Fe₃O₄), 12 nm (Fe₃O₄@SiO₂), and 10 nm (Fe₃O₄@SiO₂-SO₃H), proving the mesoporous structure of the prepared materials (Figure 1a,d). Comparison of the morphology and size distribution of the particles shows that on going from Fe₃O₄ to Fe₃O₄@SiO₂-SO₃H MNPs, the porosity of magnetic material is dramatically increased, whereas, in contrast, the size of nanoparticles tends toward a smaller range. This is attributed to carrying out more processes on the magnetite cores (layering of SiO₂ followed by the immobilization of sulfonic acid moiety). Because of this, making additional shells decreases the magnetic property of the Fe₃O₄ nucleus to attract the others for agglomeration.

EDX is a useful technique to determine the elemental profile of materials. The EDX spectrum of sulfonated silica-layered magnetite shows the presence of Fe, O, Si, and S elements, demonstrating the successful synthesis of Fe₃O₄@SiO₂-SO₃H MNPs (Figure 2).

Next, XRD patterns of Fe₃O₄, Fe₃O₄@SiO₂, and Fe₃O₄@SiO₂-SO₃H MNPs were used for their structural analysis. Figure 3a shows the diffraction peaks at 2θ values of 30.2°, 35.5°, 43.3°, 53.7°, 57.2°, and 62.9° corresponding
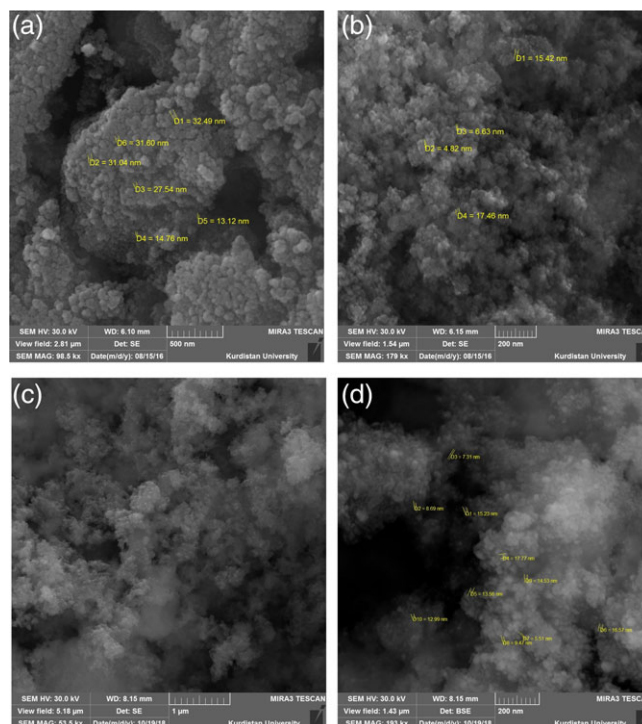

FIGURE 1 SEM images of (a) Fe₃O₄, (b) Fe₃O₄@SiO₂, and (c,d) Fe₃O₄@SiO₂-SO₃H MNPs

SCHEME 1 Reduction of oximes with NaBH₃CN under solvent-free conditions

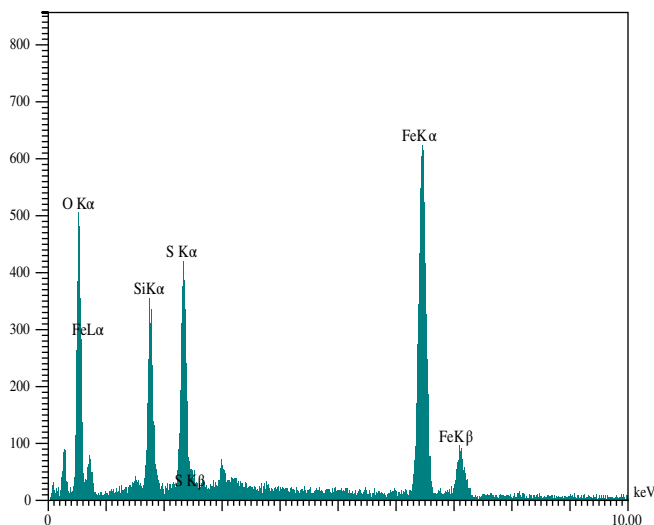**FIGURE 2** EDX spectrum of $Fe_3O_4@SiO_2$-SO_3H MNPs

to the (220), (311), (400), (422), (511), and (440) crystal planes of Fe_3O_4. The obtained magnetite has crystalline cubic spinel structure, which is in good agreement with that of the standard Fe_3O_4 (JCPDS 65-3107). Accordingly, the XRD patterns of $Fe_3O_4@SiO_2$ and $Fe_3O_4@SiO_2$-SO_3H MNPs also show that both patterns include all characteristic peaks of the bare magnetite (Figures 3b,c). This shows that during the layering and immobilization of SiO_2 and SO_3H, respectively, the cubic spinel structure of magnetite
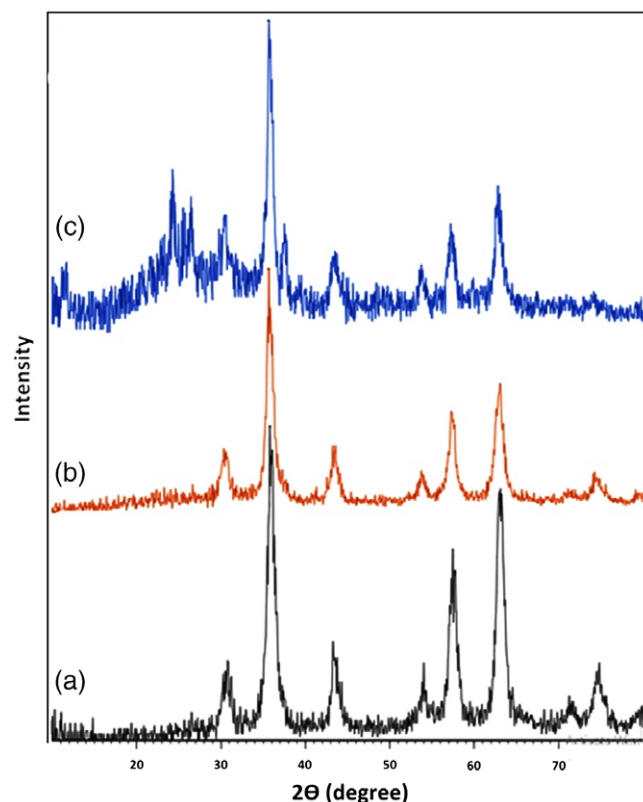
FIGURE 3 XRD patterns of (a) Fe_3O_4, (b) $Fe_3O_4@SiO_2$, and (c) $Fe_3O_4@SiO_2$-SO_3H MNPs

remained intact. In addition, a comparison of the XRD patterns of Fe_3O_4, $Fe_3O_4@SiO_2$, and $Fe_3O_4@SiO_2$-SO_3H MNPs shows that through the immobilization of sulfonic acid moiety on the surface of $Fe_3O_4@SiO_2$ MNPs, based on diminishing the sharpness of signals and the appearance of a broad absorption peak at $2\theta = 24$–$26°$, the crystallinity of $Fe_3O_4@SiO_2$-SO_3H MNPs has decreased. It means that there is a small amorphous phase in the sulfonated nanocomposite.[35] The average crystallite size for $Fe_3O_4@SiO_2$-SO_3H MNPs was calculated as 11.84 nm by Scherrer's equation using the peak at $2\theta = 35.5°$ (Figure 3c).

Structural elucidation of MNPs was also carried out by the analysis of the recorded FT-IRs. Figure 4a shows the FT-IR spectrum of Fe_3O_4 MNPs. In this spectrum, the absorption bands at around 1,623 and 3,408 cm^{-1} are assigned to the O–H deformation and stretching vibrations of the adsorbed water, respectively. The band appearing at 572 cm^{-1} is also attributed to the vibration of Fe–O bond. The FT-IR spectrum of $Fe_3O_4@SiO_2$ MNPs is shown in Figure 4b. The spectrum shows absorption peaks at around 798 and 1,086 cm^{-1}, corresponding to the symmetric and asymmetric stretching vibration of Si–O–Si. In Figure 4c, the bands at around 1,197 and 1,130 cm^{-1} are, respectively, attributed to the asymmetric and symmetric stretching vibration of SO_2. In this context, the absorption band corresponding to the symmetric stretching of SO_2 (1,130 cm^{-1}) is overlapped with a wide and strong absorption peak due to the Si–O bond (1,081 cm^{-1}). Moreover, the absorption peaks at around 656 and 3,390 cm^{-1} are related to the S–OH and O–H stretching vibration of sulfonic acid and water molecules, respectively. Based on these results, the successful immobilization of sulfonic acid moiety as well as layering of SiO_2 on the magnetite nucleus is demonstrated.

More investigations on the magnetic property of Fe_3O_4, $Fe_3O_4@SiO_2$ and $Fe_3O_4@SiO_2$-SO_3H MNPs were also carried out by the VSM technique under an applied external magnetic field of up to 20 kOe (Figure 5). The saturation magnetization (M_s) values of Fe_3O_4, $Fe_3O_4@SiO_2$, and $Fe_3O_4@SiO_2$-SO_3H were 67, 29, and 19.68 emu/g, respectively. It is clear that through the layering of silica, followed

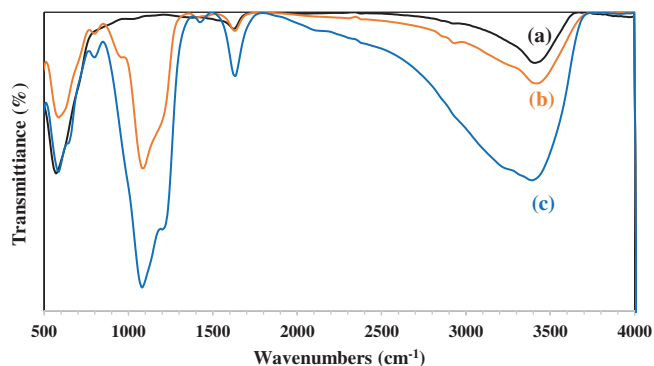**FIGURE 4** FT-IR spectra of (a) Fe_3O_4, (b) $Fe_3O_4@SiO_2$, and (c) $Fe_3O_4@SiO_2$-SO_3H MNPs
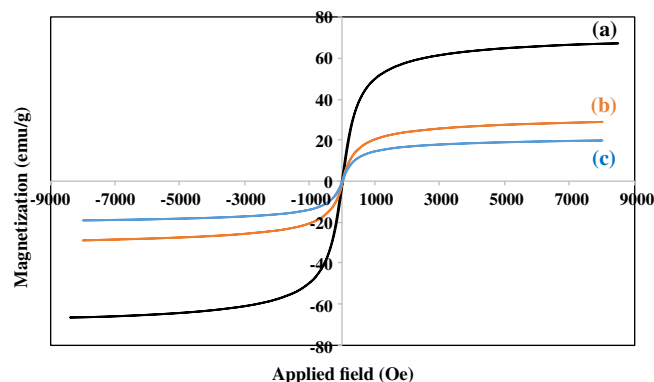
FIGURE 5 Magnetization curves of (a) Fe_3O_4, (b) $Fe_3O_4@SiO_2$, and (c) $Fe_3O_4@SiO_2$-SO_3H MNPs

by the immobilization of sulfonic acid moiety on the cores of magnetite, the magnetization value is diminished. However, it is sufficient for any magnetic separation.

In continuation, from the TEM images of sulfonated silica-layered magnetite, the synthesis of $Fe_3O_4@SiO_2$-SO_3H MNPs in the core–shell form was also demonstrated (Figure 6).

The influence of acidity of $Fe_3O_4@SiO_2$-SO_3H MNPs on the reducing ability of $NaBH_3CN$ was then investigated through the reduction of oximes. To optimize the reaction conditions, we carried out the reduction of benzaldehyde oxime as a model compound with $NaBH_3CN$ in the absence and presence of nano-$Fe_3O_4@SiO_2$-SO_3H (Table 1, entries 1–12). The results show that the use of solvent-free media (75–80°C) was the best choice, and significant progress of the reaction was achieved using $NaBH_3CN$ (5 mmol) and nano-$Fe_3O_4@SiO_2$-SO_3H (0.05 g) per 1 mmol of the oxime (Table 1, entry 4). Further experiments revealed that increasing the amount of $Fe_3O_4@SiO_2$-SO_3H decreased the rate of reaction. In continuation, our good experience with the

FIGURE 6 TEM images of $Fe_3O_4@SiO_2$-SO_3H MNPs

Lewis acidity of $ZrCl_4$[15] encouraged us to examine the promoter activity of $ZrCl_4$ toward the reduction of benzaldehyde oxime with the $NaBH_3CN/Fe_3O_4@SiO_2$-SO_3H system. As seen in Table 1, although $ZrCl_4$ and nano-$Fe_3O_4@SiO_2$-SO_3H did not individually affect the reduction of benzaldehyde oxime (Table 1, entries 2 and 4), the reducing ability of $NaBH_3CN$ in the presence of both $Fe_3O_4@SiO_2$-SO_3H and $ZrCl_4$ dramatically increased. More investigations showed that the use of molar equivalent of oxime/$NaBH_3CN$/$ZrCl_4$ (1:5:1) and $Fe_3O_4@SiO_2$-SO_3H MNPs (0.05 g) was the requirement for the complete reduction of benzaldehyde oxime to benzylamine within 10 min under solvent-free condition (Table 1, entry 10).

The usefulness of $NaBH_3CN/ZrCl_4$/nano-$Fe_3O_4@SiO_2$-SO_3H system was further studied with the solvent-free reduction of various aldoximes. Table 2 shows the general trend and versatility of this synthetic protocol. As seen, all aldoximes containing electron-releasing or electron-withdrawing groups were reduced easily and efficiently with 5:1 M equiv of $NaBH_3CN/ZrCl_4$ in the presence of nano-$Fe_3O_4@SiO_2$-SO_3H (0.05 g) under solvent-free conditions (75–80°C). The corresponding amines were obtained in high to excellent yields within 10–70 min.

The reactivity of ketoximes toward the $NaBH_3CN/ZrCl_4$/nano-$Fe_3O_4@SiO_2$-SO_3H system was also examined by the solvent-free reduction of acetophenone oxime under the optimized conditions. Using 5:1 M equiv of $NaBH_3CN/ZrCl_4$ and nano-$Fe_3O_4@SiO_2$-SO_3H (0.05 g) reduced 1 molar equivalent of acetophenone oxime to α-methylbenzylamine within 15 min and 90% yield (Table 3, entry 1). The reducing ability of the examined protocol was further studied by the successful reduction of various ketoximes to the corresponding primary amines (Table 3). All reactions were carried out perfectly within 3–45 min to afford amines in high yields.

Comparison of the results in Tables 2 and 3 shows that ketoximes were reduced generally faster than aldoximes. In addition, aryl aldoximes having a nitro group showed good chemoselectivity in their reductions, and only the oxime group was reduced during the progress of the reaction. In the case of aryl ketoximes with the substituted nitro group, the protocol was not selective, and both oxime and nitro groups were reduced with the same reactivity (Table 2, entries 5, 6; Table 3, entry 6).

The possibility of recycling the nanocatalyst was also examined in the reduction of benzaldehyde oxime with the $NaBH_3CN/ZrCl_4$/$Fe_3O_4@SiO_2$-SO_3H MNPs system. After completion of the reaction, the magnetic nanoparticles of $Fe_3O_4@SiO_2$-SO_3H were separated from the reaction mixture by an external magnet and then reused (after washing with distilled water/acetone and dried under vacuum) for the next runs. The recycled nanocatalyst could be reused at least three times without any significant loss of its catalytic activity (Figure 7).
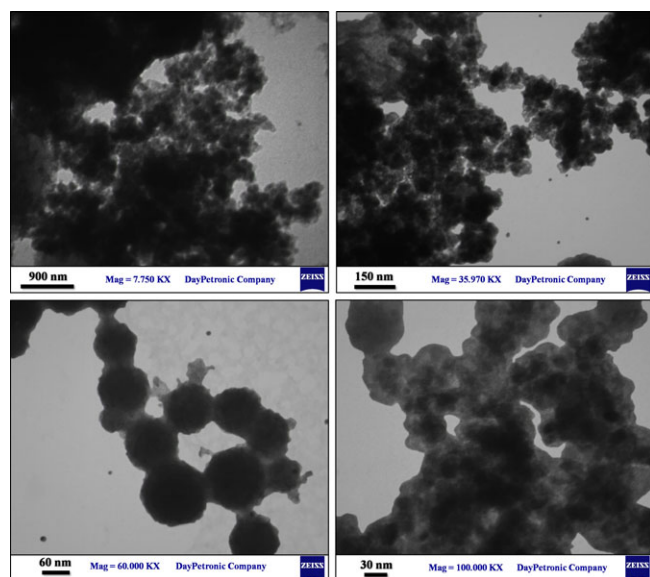
TABLE 1 Optimization experiments for the reduction of benzaldehyde oxime to benzylamine with the NaBH$_3$CN/ ZrCl$_4$/nano-Fe$_3$O$_4$@SiO$_2$-SO$_3$H system

Entry	Reaction components (molar ratio)	Catalyst (g)	Condition[a]	Time (min)	Conv. (%)[b]
1	Oxime/NaBH$_3$CN (1:5)	—	Solvent-free/oil bath	120	0
2	Oxime/NaBH$_3$CN/ZrCl$_4$ (1:5:1)	—	Solvent-free/oil bath	120	20
3	Oxime/NaBH$_3$CN (1:5)	0.05	Solvent-free/rt	60	0
4	Oxime/NaBH$_3$CN (1:5)	0.05	Solvent-free/oil bath	60	40
5	Oxime/NaBH$_3$CN (1:5)	0.1	Solvent-free/oil bath	60	30
6	Oxime/NaBH$_3$CN (1:5)	0.05	CH$_3$CN/reflux	120	0
7	Oxime/NaBH$_3$CN (1:5)	0.05	THF/reflux	120	0
8	Oxime/NaBH$_3$CN/ZrCl$_4$ (1:5:2)	0.1	Solvent-free/oil bath	10	Mix.
9	Oxime/NaBH$_3$CN/ZrCl$_4$ (1:5:1)	0.1	Solvent-free/oil bath	30	90
10	Oxime/NaBH$_3$CN/ZrCl$_4$ (1:5:1)	0.05	Solvent-free/oil bath	10	100
11	Oxime/NaBH$_3$CN/ZrCl$_4$ (1:5:0.5)	0.05	Solvent-free/oil bath	60	60
12	Oxime/NaBH$_3$CN/ZrCl$_4$ (1:5:1)	0.04	Solvent-free/oil bath	60	80
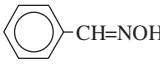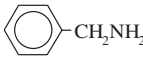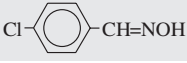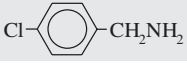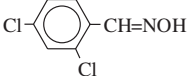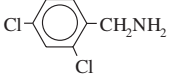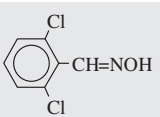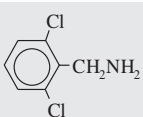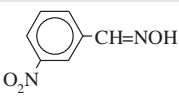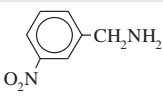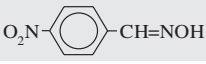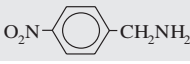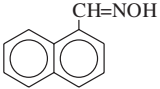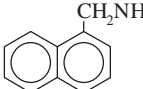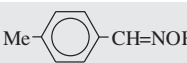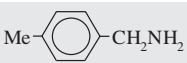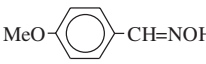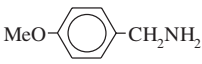
[a] Temperature of oil bath was 75–80°C.
[b] Mix. means mixture of products.

2.1 | Conclusion

In this work, we prepared magnetic nanoparticles of sulfonated silica-layered magnetite and then characterized them using SEM, EDX, XRD, FT-IR, VSM, and TEM analyses. The core–shell nanocomposite showed excellent catalytic activity in the successful reduction of various aldoximes and ketoximes to the corresponding amines with the NaBH$_3$CN/ZrCl$_4$ system. All reactions were carried out
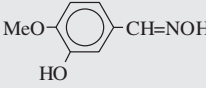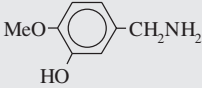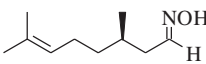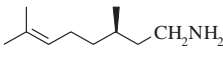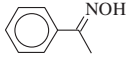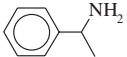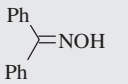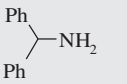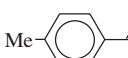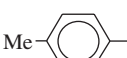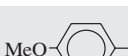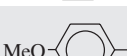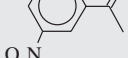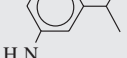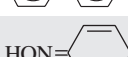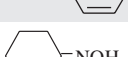
TABLE 2 Reduction of aldoximes with the NaBH$_3$CN/ZrCl$_4$/nano-Fe$_3$O$_4$@SiO$_2$-SO$_3$H system[a]

Entry	Substrate	Product (a)	Molar ratio[b]	Time (min)	Yield (%)[c]	Bp or Mp (°C)[37–41]
1	C$_6$H$_5$-CH=NOH	C$_6$H$_5$-CH$_2$NH$_2$	1:5:1	10	93	185@760 mmHg
2	Cl-C$_6$H$_4$-CH=NOH	Cl-C$_6$H$_4$-CH$_2$NH$_2$	1:5:2	70	90	217@760 mmHg
3	Cl,Cl-C$_6$H$_3$-CH=NOH	Cl,Cl-C$_6$H$_3$-CH$_2$NH$_2$	1:5:1	45	87	221@760 mmHg
4	Cl,Cl-C$_6$H$_3$-CH=NOH	Cl,Cl-C$_6$H$_3$-CH$_2$NH$_2$	1:5:1	50	89	252@760 mmHg
5	O$_2$N-C$_6$H$_4$-CH=NOH	O$_2$N-C$_6$H$_4$-CH$_2$NH$_2$	1:5:2	50	90	295@760 mmHg
6	O$_2$N-C$_6$H$_4$-CH=NOH	O$_2$N-C$_6$H$_4$-CH$_2$NH$_2$	1:5:1	50	90	298@760 mmHg
7	naphthalene-CH=NOH	naphthalene-CH$_2$NH$_2$	1:5:1	20	83	291@760 mmHg
8	Me-C$_6$H$_4$-CH=NOH	Me-C$_6$H$_4$-CH$_2$NH$_2$	1:5:1	20	92	195@760 mmHg
9	MeO-C$_6$H$_4$-CH=NOH	MeO-C$_6$H$_4$-CH$_2$NH$_2$	1:5:1	30	90	237@760 mmHg
10	MeO,HO-C$_6$H$_3$-CH=NOH	MeO,HO-C$_6$H$_3$-CH$_2$NH$_2$	1:5:1	15	88	193–195
11	citronellal oxime (=NOH, H)	citronellal amine (CH$_2$NH$_2$)	1:5:1	20	86	219@760 mmHg

[a] All reactions were carried out in the presence of nano-Fe$_3$O$_4$@SiO$_2$-SO$_3$H (0.05 g) in an oil bath (75–80°C) under solvent-free conditions.
[b] Molar ratio as: Subs./NaBH$_3$CN/ZrCl$_4$.
[c] Yields refer to isolated pure products.

TABLE 3 Reduction of ketoximes with the NaBH$_3$CN/ZrCl$_4$/nano-Fe$_3$O$_4$@SiO$_2$-SO$_3$H system[a]

Entry	Substrate	Product (b)	Molar ratio[b]	Time (min)	Yield (%)[c]	Bp or Mp (°C)[37–41]
1			1:5:1	15	90	186@760 mmHg
2			1:5:1	40	87	300@760 mmHg
3			1:5:1	45	93	208@760 mmHg
4			1:5:1	20	90	240@760 mmHg
5			1:5:1	30	88	82@2.8 mmHg
6			1:5:1	20	86	55–58
7			1:5:1	20	96	328@760 mmHg
8[d]			1:5:1	5	92	138–145
9[d]			1:5:1	3	83	134@760 mmHg
10[d]			1:5:1	5	85	279@760 mmHg

[a] All reactions were carried out in the presence of nano-Fe$_3$O$_4$@SiO$_2$-SO$_3$H (0.05 g) in an oil bath (75–80°C) under solvent-free conditions.
[b] Molar ratio as: Subs./NaBH$_3$CN/ZrCl$_4$.
[c] Yields refer to isolated pure products.
[d] The reaction was carried out at r.t.

within 3–70 min under solvent-free conditions (r.t. or 75–80°C), affording the product amines in high to excellent yields. Clean reactions, short reaction times, reusability of the nanocatalyst, easy work-up procedure, high yield of products, solvent-free conditions, and using Fe$_3$O$_4$@SiO$_2$-SO$_3$H MNPs as a solid-acid catalyst for NaBH$_3$CN reduction of oximes rather than using strong aqueous acidic media are the advantages of this method, which make the current protocol a synthetically useful addition to the present methodologies.

FIGURE 7 Reusability of Fe$_3$O$_4$@SiO$_2$-SO$_3$H MNPs in the reduction of benzaldehyde oxime

3 | EXPERIMENTAL

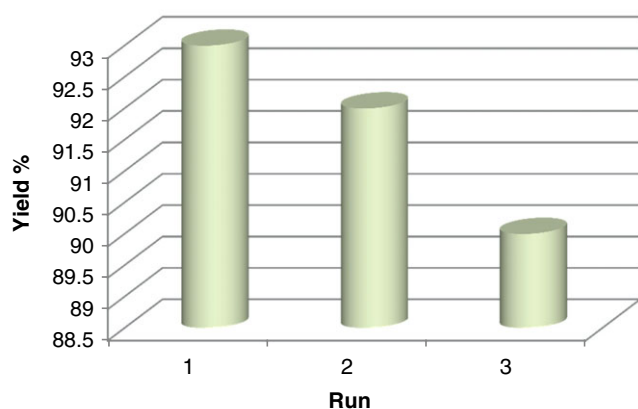All reagents and solvents were purchased from Merck with high quality and used without further purification. Oximes were prepared in high purity according to the reported procedures.[36] ^{1}H and ^{13}C NMR spectra were recorded with a 300-MHz Bruker spectrometer at room temperature with CDCl$_3$ as solvent. The FT-IR spectra were recorded on a Thermo Nicolet Nexus 670 FT-IR spectrometer. The XRD data were collected using a Philips X'pert Pro diffractometer using Cu Kα radiation ($2\theta = 10°–80°$, $\lambda = 1.54056$ Å). The surface morphology of the particles was assigned by SEM using an FESEM-TESCAN MIRA3 instrument. The chemical composition of Fe$_3$O$_4$@SiO$_2$-SO$_3$H MNPs was determined using EDX. The magnetic property of the materials was determined using a vibrating sample magnetometer under magnetic fields up to 20 kOe. TEM was carried out on a Zeiss-EM10C instrument operated at 100 kV. An ultrasonic bath with temperature control (FALC, model LBS2) was used for sonication. TLC was used for the purity determination of substrates, products, and reaction monitoring, over silica gel 60 F$_{254}$ aluminum sheet. All products are known and so were characterized by comparison of their spectra and physical data with those available in the literature.[37–41]

3.1 | Preparation of $Fe_3O_4@SiO_2$-SO_3H MNPs

Magnetic nanoparticles of Fe_3O_4 were prepared via the chemical co-precipitation of Fe^{2+} and Fe^{3+} ions in an alkali medium.[42] The particles were subsequently coated with a silica layer ($Fe_3O_4@SiO_2$)[43] and then functionalized with sulfonic acid through reported procedures.[33,34] The prepared nanoparticles of $Fe_3O_4@SiO_2$ (1 g) were dispersed in dry CH_2Cl_2 (10 mL) by ultrasonication for 30 min. Subsequently, $ClSO_3H$ (1 mL) was added dropwise to a cooled mixture of $Fe_3O_4@SiO_2$ (ice bath) within 30 min at room temperature. After the addition, the mixture was stirred for 6 hr to complete the extrusion of HCl. The resulting magnetic nanoparticles were separated using an external magnet and washed with ethanol and water before drying in an oven at 70°C to give $Fe_3O_4@SiO_2$-SO_3H MNPs as a brown powder. The number of H^+ sites (0.31 mmol/g) was determined by acid–base titration.[44]

3.2 | Typical procedure for the solvent-free reduction of benzaldehyde oxime to benzylamine with the $NaBH_3CN$/ $ZrCl_4$/$Fe_3O_4@SiO_2$-SO_3H MNP system

A mixture of benzaldehyde oxime (0.121 g, 1 mmol) and nano-$Fe_3O_4@SiO_2$-SO_3H (0.05 g) was ground in a porcelain mortar. $ZrCl_4$ (0.233 g, 1 mmol) was then added, and grinding was continued for a while at r.t. The mortar was heated in an oil bath to keep the temperature at 75–80°C. $NaBH_3CN$ (0.314 g, 5 mmol) was then added portion-wise, and the mixture was ground for 10 min in an oil bath (75–80°C). After completion of the reaction, H_2O (5 mL) was added and the mixture was stirred for 5 min. The mixture was extracted with EtOAc (2 × 5 mL) (all nano-$Fe_3O_4@SiO_2$-SO_3H remained around the stirring bar) and then dried over anhydrous Na_2SO_4. Evaporation of the solvent afforded the pure liquid benzylamine in 93% yield (0.1 g, Table 2, entry 1).

3.3 | Spectral data for selected products

3.3.1 | Benzylamine (1a)

FT-IR (KBr, v cm^{-1}) 3,368, 3,292, 3,061, 3,026, 2,920, 2,858, 1,605, 1,452; ^1H NMR (300 MHz, CDCl$_3$) δ 1.51 (s, 2H, NH$_2$), 3.87 (s, 2H, CH$_2$), 7.23–7.38 (m, 5H, Ph-H); ^{13}C NMR (75 MHz, CDCl$_3$) δ 46.54, 126.76, 127.05, 128.53, 143.37.

3.3.2 | 2,4-Dichlorolbenzylamine (3a)

FT-IR (KBr, v cm^{-1}) 3,349, 3,215, 3,038, 2,963, 1,600, 1,499, 1,278, 965, 800, 778, 692; ^1H NMR (300 MHz, CDCl$_3$) δ 1.58 (s, 2H, NH$_2$), 3.91 (s, 2H, CH$_2$), 7.25–7.38 (m, 3H, Ph-H); ^{13}C NMR (75 MHz, CDCl$_3$) δ 43.90, 127.28, 129.29, 129.72.

3.3.3 | α-Methylbenzylamine (1b)

FT-IR (KBr, v cm^{-1}) 3,293, 3,259, 1,663, 1,435, 1,179, 1,040, 961, 743; ^1H NMR (300 MHz, CDCl$_3$) δ 1.41 (d, J = 6.6 Hz, 3H, CH$_3$), 1.83 (s, 2H, NH$_2$), 4.12 (q, J = 6.6 Hz, 1H, CH), 7.19–7.39 (m, 5H, Ph-H); ^{13}C NMR (75 MHz, CDCl$_3$) δ 29.68, 51.33, 125.37, 125.71, 126.90, 128.51.

3.3.4 | Diphenylmethylamine (2b)

FT-IR (KBr, v cm^{-1}) 3,430, 3,354, 3,214, 3,005, 1,600, 1,496, 1,278, 1,174, 762, 692; ^1H NMR (300 MHz, CDCl$_3$) δ 3.65 (bs, 2H, NH$_2$, exchangeable with D$_2$O), 4.77 (s, 1H, CH), 7.27–7.48 (m, 10H, 2Ph-H); ^{13}C NMR (75 MHz, CDCl$_3$) δ 59.74, 126.90, 126.95, 128.47, 145.55.

3.3.5 | α-Methyl-4-methylbenzylamine (3b)

FT-IR (KBr, v cm^{-1}) 3,349, 3,215, 3,038, 1,600, 1,499, 1,278, 985, 753; ^1H NMR (300 MHz, CDCl$_3$) δ 1.39 (d, J = 6.6 Hz, 3H, CH$_3$), 2.06 (s, 2H, NH$_2$), 2.34 (s, 3H, CH$_3$), 4.09 (q, J = 6.6 Hz, 1H, CH), 7.14–7.27 (m, 4H, Ph-H); ^{13}C NMR (75 MHz, CDCl$_3$) δ 25.47, 29.68, 51.01, 125.60, 129.14, 136.42, 144.45.

3.3.6 | 4-Chloro-α-methylbenzylamine (5b)

FT-IR (KBr, v cm^{-1}) 3,430, 3,354, 3,214, 1,602, 1,468, 1,276, 752; ^1H NMR (300 MHz, CDCl$_3$) δ 1.35 (d, J = 6.6 Hz, 3H, CH$_3$), 1.75 (s, 2H, NH$_2$), 4.10 (q, J = 6.6 Hz, 1H, CH), 6.98–7.41 (m, 4H, Ph-H); ^{13}C NMR (75 MHz, CDCl$_3$) δ 29.68, 50.71, 127.14, 128.53, 132.35, 146.04.

3.3.7 | α-Methyl-3-nitrobenzylamine (6b)

FT-IR (KBr, v cm^{-1}) 3,347, 3,275, 2,923, 1,605, 1,535, 1,345, 840; ^1H NMR (300 MHz, CDCl$_3$) δ 1.42 (d, J = 5.8 Hz, 3H, CH$_3$), 1.81 (bs, 2H, NH$_2$), 4.25 (q, J = 5.8 Hz, 1H, CH), 7.10–8.24 (m, 4H, Ph-H); ^{13}C NMR (CDCl$_3$, 75 MHz) δ 38.47, 53.41, 110.14, 114.58, 120.86, 121.87, 129.35, 132.19.

ORCID

Leila Sadighnia https://orcid.org/0000-0001-6433-2352
Behzad Zeynizadeh https://orcid.org/0000-0003-0485-5455

REFERENCES

[1] P. G. Andersson, I. J. Munslow, *Modern Reduction Methods*, Wiley-VCH, New York **2008**.

[2] S. D. Burke, R. L. Danheiser, *Handbook of Reagents for Organic Synthesis, Oxidizing and Reducing Agents*, Wiley-VCH, New York **1999**.

[3] A. F. Abdel-Magid, *Reductions in Organic Synthesis*. ACS Symposium Series 641, ACS Publications, Washington, DC **1996**.

[4] M. Hudlicky, *Reductions in Organic Chemistry*, Ellis Horwood, Chichester **1984**.

[5] L. Banfi, E. Narisano, R. Riva, N. Stiasni, M. Hiersemann, in *Encyclopedia of Reagents for Organic Synthesis* (Ed: L. Paquette), Wiley, New York **2004**.

[6] J. Seyden-Penne, *Reductions by the Alumino and Borohydrides in Organic Synthesis*, 2nd ed., Wiley-VCH, New York **1997**.

[7] C. F. Lane, *Synthesis* **1975**, *3*, 135.

[8] R. O. Hutchins, I. M. Taffer, W. Burgoyne, *J. Org. Chem.* **1981**, *46*, 5214.

[9] S. Kim, C. H. Oh, J. S. KO, K. H. Ahn, Y. J. Kim, *J. Org. Chem.* **1927**, *1985*, 50.

[10] O. Han, Y. Shih, L. Liu, H. Liu, *J. Org. Chem.* **1988**, *53*, 2105.

[11] L. A. Paquette, D. Crich, P. L. Fuchs, G. A. Molander, *Encyclopedia of Reagents for Organic Synthesis*, 2nd ed., Wiley-VCH, Weinheim **2009**.

[12] R. C. Larock, *Comprehensive Organic Transformations: A Guide to Functional Group Preparations*, 2nd ed., Wiley-VCH, Weinheim **2010**.

[13] R. F. Borch, M. D. Bernstein, H. D. Durst, *J. Am. Chem. Soc.* **1971**, *93*, 2897.

[14] R. O. Hutchins, D. Kandasamy, *J. Org. Chem.* **1975**, *40*, 2530.

[15] L. Sadighnia, B. Zeynizadeh, *J. Iran. Chem. Soc.* **2015**, *12*, 873.

[16] A. Ricci, *Modern Amination Methods*, Wiley-VCH, Weinheim **2000**.

[17] H. U. Blaser, C. Malan, B. Pugin, F. Spindler, H. Steiner, M. Studer, *Adv. Synth. Catal.* **2003**, *345*, 103.

[18] S. A. Lawrence, *Amines: Synthesis, Properties and Applications*, Cambridge University Press, Cambridge **2004**.

[19] T. C. Nugent, *Chiral Amine Synthesis: Methods, Developments and Applications*, Wiley-VCH, Weinheim **2010**.

[20] T. Farooqui, A. A. Farooqui, *Biogenic Amines: Pharmacological, Neurochemical and Molecular Aspects in the CNS*, Nova Science Publisher, Hauppauge **2010**.

[21] J. Hagen, *Industrial Catalysis: A Practical Approach*, 2nd ed., Wiley-VCH, Weinheim **2006**.

[22] H. J. Arpe, *Industrial Organic Chemistry*, 5th ed., Wiley-VCH, Weinheim **2010**.

[23] R. B. N. Baig, R. S. Varma, *Green Chem.* **2012**, *14*, 625.

[24] N. Koukabi, E. Kolvari, A. Khazaei, M. A. Zolfigol, B. Shirmardi-Shaghasemi, H. R. Khavas, *Chem. Commun.* **2011**, *47*, 9230.

[25] R. S. Varma, *Sustain. Chem. Process.* **2014**, *2*, 11.

[26] M. B. Gawande, A. K. Rathi, P. S. Branco, R. S. Varma, *Appl. Sci.* **2013**, *3*, 656.

[27] M. B. Gawande, P. S. Branco, R. S. Varma, *Chem. Soc. Rev.* **2013**, *42*, 3371.

[28] R. B. N. Baig, R. S. Varma, *Green Chem.* **2013**, *15*, 398.

[29] Z. W. Li, Y. F. Zhu, *Appl. Surf. Sci.* **2003**, *211*, 315.

[30] H. Younes, G. Christensen, X. N. Luan, H. D. Hong, P. Smith, *J. Appl. Phys.* **2012**, *111*, 64308.

[31] Y. Lin, H. Chen, K. Lin, B. Chen, C. Chiou, *J. Environ. Sci.* **2011**, *23*, 44.

[32] N. M. Mahmoodi, S. Khorramfar, F. Najafi, *Desalination* **2011**, *279*, 61.

[33] H. Naeimi, Z. S. Nazifi, *J. Nanopart. Res.* **2013**, *15*, 2026.

[34] J. Safari, Z. Zarnegar, *J. Mol. Catal. A: Chem.* **2013**, *379*, 269.

[35] F. Nemati, S. Sabaqian, *J. Saudi Chem. Soc.* **2017**, *21*, S383.

[36] B. Zeynizadeh, E. Amjadi, *Asian J. Chem.* **2009**, *21*, 3611.

[37] Global Chemical Network, http://www.chemnet.com (accessed: January 2018).

[38] Sigma Aldrich. Sigma Aldrich online catalogue. http://www.sigmaaldrich.com (accessed: January 2018).

[39] Integrating Global Trade Leads. http://www.weiku.com (accessed: January 2018).

[40] Acros Organics. http://www.acros.com (accessed: January 2018).

[41] OXchem. http://demo.xmlsite.cn/ark/web/index.html (accessed: January 2018).

[42] E. Rafiee, S. Eavani, *Green Chem.* **2011**, *13*, 2116.

[43] D. Yang, J. Hu, S. Fu, *J. Phys. Chem. C.* **2009**, *113*, 7646.

[44] F. Nemati, M. M. Heravi, R. Saeedi Rad, *Chin. J. Catal.* **2012**, *33*, 1825.